Brittle failures of connections with self-tapping screws on CLT plates

Cabrero, José Manuel; Niederwestberg, Jan; Azinović, Boris; Danielsson, Henrik; Ying Hei Chui; Pazlar, Tomaž; Chun Ni

Published in:
Proceedings of the International Network on Timber Engineering Research - INTER

2022

Document Version:
Peer reviewed version (aka post-print)

Brittle failures of connections with self-tapping screws on CLT plates

José M. Cabrero, ONESTA Wood Chair. University of Navarra, 31009 Pamplona, Spain. jcabrero@unav.es

Jan Niederwestberg, University of Alberta, Faculty of Engineering, Edmonton, AB T6G 2R3, Canada. niederwe@ualberta.ca

Boris Azinović, Slovenian National Building and Civil Engineering Institute (ZAG Ljubljana), 1000 Ljubljana, Slovenia. boris.azinovic@zag.si

Henrik Danielsson, Lund University, Faculty of Engineering LTH, 221 00 Lund, Sweden. henrik.danielsson@construction.lth.se

Ying Hei Chui, University of Alberta, Faculty of Engineering, Edmonton, AB T6G 2R3, Canada. yhc@ualberta.ca

Tomaž Pazlar, Slovenian National Building and Civil Engineering Institute (ZAG Ljubljana), 1000 Ljubljana, Slovenia. tomaz.pazlar@zag.si

Chun Ni, FPInnovations, Canada, chun.ni@fpinnovations.ca

Keywords: Timber connection, Brittle failure, Cross Laminated Timber, Parallel-to-grain, Self-tapping screws, Eurocode 5 , CSAO86

1 Introduction

Cross Laminated Timber (CLT) has become a popular product in current timber construction. However, several features set it aside from typical timber products, namely due to its crosswise layer arrangement. Regarding its failure response, the perpendicular layers are supposed to provide dimensional stability and reinforcement. Hence, it is sometimes assumed that brittle failure may be greatly reduced.

However, as shown in previous works by *Zarnani and Quenneville* (2015) and *Asgari et al.* (2022), this is not necessarily the case.

In the European context, as CLT is not yet included as a product in the current Eurocode 5, CLT connection design is yet to be included. Practitioners (*Schenk et al.*, 2022) use several manuals (*Wallner-Novak et al.*, 2014; *Borgström and Fröbel*, 2019; *Bogensperger et al.*, 2010) and ETAs from CLT and fastening manufacturers (*ETA 12-0347*, 2020; *ETA 14-0349*, 2020).

CLT design is already taken into account in the US (*ASTM D5457-21a*, 2021) and Canadian regulations (*CSA O86-09*, 2019). In the latter, as pointed out by *Asgari et al.* (2022), a statement is given where row shear and group tear out (block or plug shear) are explicitly dismissed in CLT connections. On the other hand, in the current Eurocode 5 draft, a note regarding the possibility of brittle failure was discussed in the commenting process, but no guidance is eventually given.

Brittle failure in connections could become a problem if the designer is not able to consider it, for two main reasons: reduction of ductility in cases where the structural design demands it, or reduction of estimated load-carrying capacity.

Current existing brittle failure models are mainly developed for timber products such as glulam and LVL (*Cabrero and Yurrita*, 2018; *Yurrita, Cabrero, and Moreno-Zapata*, 2021; *Yurrita and Cabrero*, 2020). Due to the load distribution between adjacent layers within a CLT element, i.e. through cross-layer reinforcements, these models cannot be applied directly to CLT. *Zarnani and Quenneville* (2015) made some modifications to their original model (*Zarnani and Quenneville*, 2014) to adapt it for CLT, and verified the new approach for rivetted CLT connections.

The typical connection in CLT structures is a 3D steel plate (ie, hold-down or steel angle bar) connected to the CLT elements using small diameter fasteners, such as screws, anchor bolts or rivets. Thus, the expected brittle failure mode is plug shear, defined by three different planes: head tensile, lateral shear and bottom shear, determined by the boundary of the connection area.

Zarnani and Quenneville (2015) defined six different modes for plug shear in CLT, as shown in Figure 1. They were distinguished since different load distribution phenomena and considerations have to be introduced in the model, based on the considered penetration of the fastener in the layers.

Other failure modes different from plug shear may also appear: step shear, in which the torn block corresponds to the entire width of the panel, and the net tension failure of the complete CLT cross-section (Figure 1).

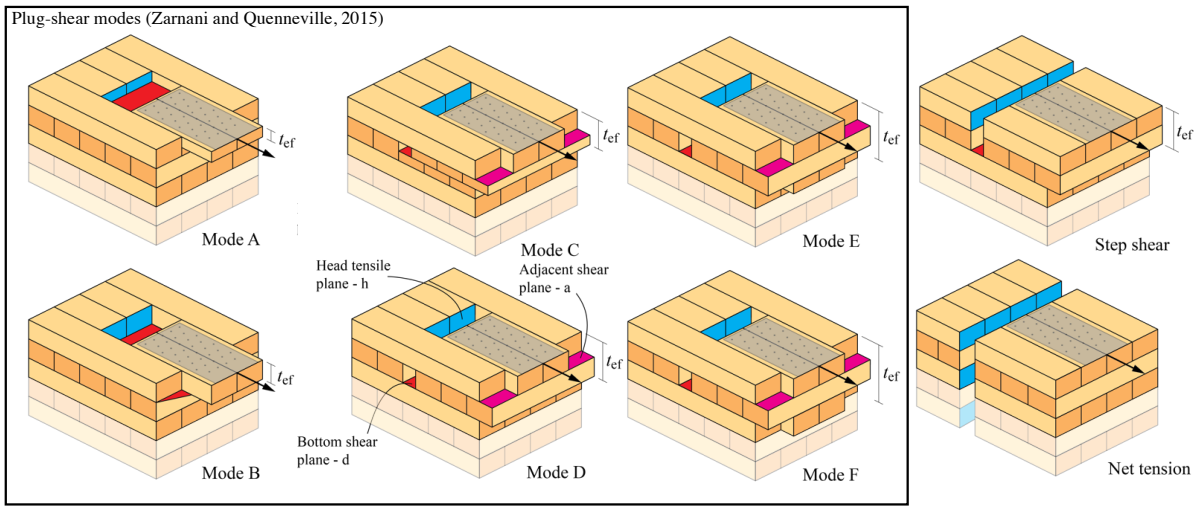

Figure 1. Typical brittle failure modes in CLT, with failure planes depicted. Plug-shear modes A-F correspond to those defined by Zarnani and Quenneville (2015).

The current paper describes two different experimental campaigns, which were carried out independently in Europe and Canada, on connections with self-tapping screws subjected to tensile loads parallel to the outer layer of the CLT. Both experimental campaigns, the obtained results and observed failure modes are described in Section 2. Sect. 3 describes briefly the existing model, its application to the performed tests and the obtained results.

2 Experimental campaigns

2.1 Europe

The European connections consisted of a single steel plate attached to both ends of a CLT element (single shear plane). It comprised ten different sets of tests (see Table 1) which differed in terms of CLT type, CLT width (w), and fastener length (ℓ_f = 40, 60, and 100 mm). Fully threaded screws with a diameter of 8 mm ($M_{y,k}$ = 20Nm according to the producer (*ETA 11-0284*, 2019)) and steel plates with dimensions 208 × 800 × 8 mm (steel grade S355) were used, with the hole pattern designed according to the provisions of Eurocode 5 (Fig. 2a). Some additional specimens (not described in this paper) were tested with the outer layer oriented perpendicular to the applied load. The interested reader may find them in the related paper (*Azinović et al.*, 2022).

The denomination of the different test series was related to the penetration of the fastener into the layers and the failure modes denomination by *Zarnani and Quenneville* (2015) (Fig. 1). Therefore, in AB specimens only the first layer is penetrated, while in CD and EF the second and third, respectively.

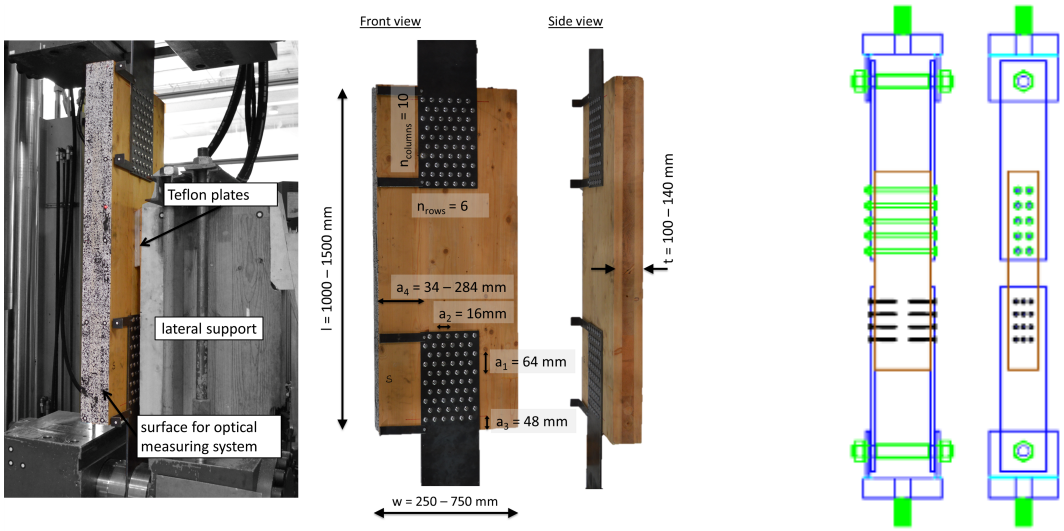

(a) Europe *(b) Canada*

Figure 2. Tests setup and used denomination for the geometrical features.

The connections were tested using a tensile test configuration (Fig. 2a) with nominally equal connections on both sides of the specimen and a displacement control protocol according to *EN 26891* (1992). The relative displacement of each connection was determined as the difference between the displacement of the steel plate and the displacement at the centre of the CLT specimen.

2.2 Canada

The Canadian data set consisted of nine steel-wood-steel connections with steel plates on both sides of the CLT element (double shear plane) with self-tapping screws (STS) (see Table 1), from the same type and manufacturer as the European ones (*ETA 11-0284*, 2019). Specimens consisted of an element of CLT, two identical STS connections and one stronger bolted connection (Fig. 2b). Bolted connections were over-designed in order to prevent their failure. All specimens were loaded parallel to the grain of the outer layers of the CLT. The spacing, end and edge distances of the STS groups followed the proposed design prescriptions.

The CLT was of V2M1.1 grade from Structurlam using SPF #2 and better lumber in all layers. The steel plates used in the tests had a thickness of 12.5 mm and a grade of 300W. The plates had pre-drilled holes in accordance with the spacings presented in Table 1. Holes for STS and bolt connections were drilled prior to installation of the steel plates. For STS connections, holes were drilled at 70% of the nominal diameter (0.7*d*) of the respective screws.

Additionally, nine different steel-to-glulam (GLT) connections were tested, but not described in this paper. The reader is referred to the full report for further details

Table 1. Basic characteristics of the specimens used in the experiments.

Test series	n [-]	w [mm]	t [mm]	ℓ [mm]	d_f [mm]	ℓ_f [mm]	n_r [-]	n_c [-]	a_1 [mm]	a_3 [mm]	a_2 [mm]	a_4 [mm]	CLT layers [mm]
Europe													
AB1	6	245	142	1 228	8	40	6	10	64	48	16	34	40-20-20-20-40
AB2	6	250	142	1 498	8	40	6	10	64	48	16	37	33-20-33-20-33
CD1	7	250	101	988	8	40	6	10	64	48	16	37	20-20-20-20-20
CD2	7	251	101	1 201	8	60	6	10	64	48	16	37	30-40-30
CD3	6	500	101	1 199	8	60	6	10	64	48	16	162	30-40-30
CD4	6	743	101	1 198	8	60	6	10	64	48	16	283	30-40-30
CD5	6	250	140	1 200	8	60	6	10	64	48	16	35	33-20-33-20-33
EF1	4	250	100	1 000	8	100	6	10	64	48	16	35	20-20-20-20-20
EF2	6	250	140	1 200	8	100	6	10	64	48	16	35	33-20-33-20-33
EF3	3	500	140	1 200	8	100	6	10	64	48	16	165	33-20-33-20-33
Canada													
CA4	3	420	175	588	8	80	5	3	40	96	24	20.5	35-35-35-35-35
CA5	3	420	175	588	8	80	5	3	40	96	24	20.5	35-35-35-35-35
CA6	3	140	175	588	8	80	5	3	40	96	24	20.5	35-35-35-35-35
CA10	3	420	175	588	8	120	5	3	40	96	24	20.5	35-35-35-35-35
CA11	3	420	175	588	8	120	5	3	40	96	24	20.5	35-35-35-35-35
CA12	3	140	175	588	8	120	5	3	40	96	24	20.5	35-35-35-35-35
CA16	3	420	175	588	12	100	3	3	60	144	36	34	35-35-35-35-35
CA17	3	420	175	588	12	100	3	3	60	144	36	34	35-35-35-35-35
CA18	3	140	175	588	12	100	3	3	60	144	36	34	35-35-35-35-35

Legend: *n, number of replicates (in the case of the European data, the actual number of tested connetions is 2n); w, t, ℓ, width, thickness and length of the CLT panel; d_f, ℓ_f, diameter and length of the self-tapping screw; n_r, n_c, number of rows (parallel to grain) and columns (perp. to grain); a_1, a_3, spacing and end distance in the parallel direction; a_2, a_4, spacing and edge distance in the perpendicular direction.*

(*Ni and Niederwestberg*, 2022). Original denominations of the test campaign have been respected in this work for consistency with the full report.

2.3 Results

Table 2 summarises the results of the tests from both campaigns. Mean $F_{t,mean}$ and characteristic $F_{t,char}$ tensile maximum loads are given, accompanied by the corresponding coefficient of variation CoV. In the case of the European campaign, since two nominally identical connections were tested simultaneously for each specimen, but only one failed, a probabilistic model based on the Weibull distribution was used to obtain the mean and coefficient of variation (CoV). The characteristic load-bearing capacity values were calculated according to the recommendations in *EN 14358* (2016), with a normal distribution assumed. This characteristic value is highly penalised in the case of the Canadian dataset due to the low number of replicates, so they may be considered as less reliable.

Furthermore, the table presents evaluated average stiffness values obtained according to *EN 26891* (1992) as secant stiffness between 10% and 40% of the ultimate load for the specimen, and the ductility index D_f as defined in *EN 12512*

Table 2. Test results.

Test series	$F_{t,mean}$ [kN]	CoV [%]	$F_{t,char}$ [kN]	F_{yield} [kN]	u_{yield} [mm]	k_{10-40} [kN/mm]	CoV [%]	D_f [-]	CoV [%]	Failure mode [-]
Europe										
AB1	260.8	8.9	200.7	247	7.8	64.7	17.3	1.5	10.0	PS/RS
AB2	236.7	8.8	181.5	199.1	6.4	66.7	27.5	1.4	29.0	PS/RS
CD1	190.2	4.4	103.7	175.7	3.9	96.4	12.1	1.5	12.8	PS
CD2	246.7	6.7	173.5	246.7	4.1	124.1	24.4	1.5	15.0	PS
CD3	304.6	8.3	229.6	267.7	4.3	146.1	12.4	1.5	6.1	PS/RS
CD4	358.1	8.8	274.3	313.5	4.5	134.3	15.8	1.5	5.8	PS/RS
CD5	224.2	5.7	143.1	200.6	3.8	112.3	8.3	1.5	4.9	PS/RS
EF1	224.9	4.9	124.2	224.9	3.4	166.2	20.6	1.4	13.5	NT
EF2	269.1	8.6	205.1	246.0	4.0	110.5	7.0	1.6	19.7	PS/RS
EF3	286.7	11.7	229.7	282.5	4.1	173.5	27.7	2.3	44.1	PS/RS
Canada										
CA4	213.0	4.1	185.3	177.0	9.0	22.7	10.0	2.5	22.7	EYM
CA5	220.0	5.0	185.1	189.0	6.4	35.6	18.3	2.0	38.8	PS
CA6	203.0	4.7	172.6	174.0	6.5	26.7	9.8	2.6	45.4	SS
CA10	309.0	0.8	301.2	167.0	6.8	26.5	18.0	3.8	11.5	EYM
CA11	297.0	10.8	195.2	197.0	6.3	21.1	13.3	2.8	31.7	EYM
CA12	228.0	16.3	111.0	172.0	6.7	25.8	16.8	1.8	27.9	SS
CA16	236.0	4.1	205.3	273.0	149	27.3	14.9	5.0	25.5	EYM
CA17	254.0	7.7	192.1	242.0	137	24.2	15.2	5.9	18.9	EYM
CA18	253.0	8.6	184.4	275.0	143	27.4	11.4	4.4	34.9	EYM

Legend: *$F_{t,mean}$, $F_{t,char}$, mean and characteristica maximum load; F_{yield}, u_{yield}, yield load and corresponding displacement; k_{10-40}, connection stiffness; D_f, connection ductility; CoV, coeffficient of variation.*
Failure modes: *PS, plug shear; RS, row shear (tearing); NT, net tension; SS, step shear; EYM, yielding of the fastener. Where two are indicated, both are observed in some specimens of the series.*

(2016). Yield loads and associated deformations are based on the 5% stiffness offset method based on *ASTM D5764-97a* (2018). In this method, the stiffness of the load-deformation curve is determined within the linear range first, and then a line with the same slope is shifted (offset) at a displacement equal to 5% of the fastener diameter. The yield load is then determined as the load at the intersection of the 5% offset curve and the load-displacement curve or ultimate load, whatever is critical.

Table 2 also presents the associated failure mode. In some cases, a secondary failure mode is presented that was observed during the tests (sometimes failure modes differed among similar specimens).

Yield loads are lower than the ultimate load capacity in most specimens. Hence, plastic deformation of the screws occurs prior to failure in most test series, although most specimens tested eventually failed in a brittle manner. This was shown to be the case also in test campaigns for self-tapping screw connections on glulam and LVL in the past (*Yurrita and Cabrero*, 2021).

(a) Europe. AB1.

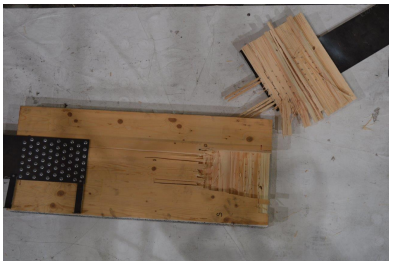

(b) Europe. CD3

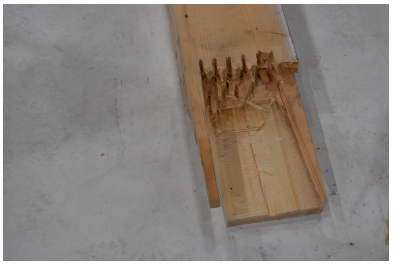

(c) Europe. EF2

(d) Canada. CA6

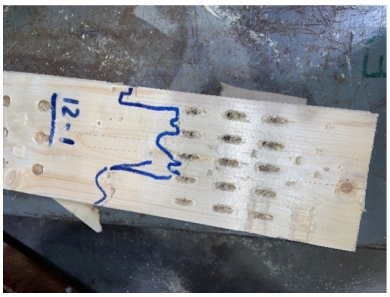

(e) Canada. CA12

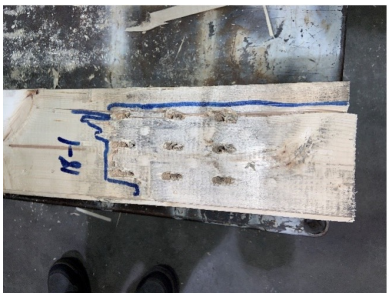

(f) Canada. CA18

Figure 3. Failures of specimens

Plug shear was the most representative failure mode, but sometimes in combination with row tearing of the screws (e.g., specimen EF2 in Fig.3c). In the case of the test series with reduced width (i.e., CA6 and CA12), due to their narrow width, the typical failure was step shear. In series EF1, net tensile failure of the CLT cross-section occurred. In the case of the Canadian dataset, some specimens eventually failed in a brittle manner, but after a significant deformation, as shown by the higher obtained ductility values. Their failure mode is marked as EYM in Table 2.

An increased specimen width increases the load-bearing capacity, while elastic stiffness does not change significantly. It is clearly observed when comparing specimens CD2 (250 mm) and CD4 (750 mm), with an increase of 45% in capacity, and a stiffness increase of only 8%. The same trend may be observed between C10 and C12 (35% capacity increase in the mean load-bearing capacity values —up to 270% at the characteristic level—, only 2% stiffness increase).

In most cases, there is a direct relationship between the fastener penetration depth and the resulting stiffness (70% increase between CD1 and EF1, with 40 mm and 100 mm). However, this trend is not so clear in the Canadian set. The increase in load capacity between comparable series with different penetration depths is not so remarkable. Although the failed timber plug is deeper for deeper fasteners, there is no significant capacity increase (e.g., AB2 and CD5).

The influence of different layups was analysed only in the case of the European campaign. No significant changes in stiffness are observed (e.g., 3% difference between AB1 and AB2, 10% between CD2 and CD5). There was a more direct influence on the resulting load capacity, mostly dependent on the penetration of the screw with respect to the individual layers.

There are significant differences in ductility between the European and Canadian series. In the case of Europe, the mean ductility was around 1.5, while it was higher in the Canadian tests, where even some tests eventually failed in a ductile way, with ductility values higher than 4 (whose failure mode is reported as EYM). One reason for this difference is response may be related to the lower number of fasteners in the Canadian set (15 screws in comparison to 60 in the European one).

3 Model verification

3.1 Model description

The model from *Zarnani and Quenneville* (2015) originates from their plug shear proposal for small diameter timber fasteners for solid wood products (*Zarnani and Quenneville*, 2014), modified to consider the crosswise layer arrangement of the CLT plates. It is a stiffness-based model, in which the total load carrying capacity is obtained by considering the stiffness of each failure plane. Hence, for every failure plane, both stiffness and capacity are defined.

The plug shear failure is defined by the failure onset of three different planes (depicted in previous Fig. 1): bottom (failing in shear), head (parallel tension) and lateral (shear). However, in the case of CLT, the lateral planes are dismissed, since in most cases boards are not laterally glued, and the position of the joints is undetermined.

In the case of the bottom plane, two different independent contributions are considered: the adjacent shear planes (a) between the top and below layers, and the bottom shear plane (d). The formulation of the bottom plane takes into account the reinforcement effect of the cross-layers that contributes to the load transfer to adjoining outer and inner parallel laminations. Due to the different occurring load distributions in relation to the fastener relative layer depth penetration, they established a set of different failure modes as shown in previous Figure 1.

After a first run of the model, a re-run to obtain the remaining capacity from the not-yet failed planes has to be additionally performed, to verify that the remaining

Table 3. Used material properties at the characteristic level (ETA 12-0347, 2020; ETA 14-0349, 2020; CSA O86-09, 2019).

Campaign	Lamination strength class	ρ_m [kg/m^3]	$E_{0,m}$ [MPa]	G_m [MPa]	$G_{m,r}$ [MPa]	$f_{t,0,k}$ [MPa]	$f_{t,90,k}$ [MPa]	$f_{v,k}$ [MPa]	$f_{v,r,k}$ [MPa]
Europe	C24	380	12 000	690	50	14	0.12	4	1.8
Canada	V2M1.1	450	10 000	600	60	19.55	0.98	2.01	0.67

capacity is not higher than the initial one. Moreover, when the fastener penetrates the second layer (Mode C), if the failure is due to the head plane, an additional resisting mechanism is defined as a virtual connection between the failed timber plug. It is obtained from the rolling shear in the bottom plane and the yielding of the fastener.

3.2 Model results

Used timber material properties are given in Table 3, obtained from typical design literature in both regions (*ETA 12-0347*, 2020; *ETA 14-0349*, 2020; *CSA O86-09*, 2019). The tensile values in the case of Canada were taken from comparable glulam values since the original ones for CLT were extremely low in comparison (for CLT, $f_{t,0,k} = 6.3$ MPa).

Obtained results are given in Table 4, which contains not only the prediction of the load capacity but also the predicted mode (based on the penetration of the fastener, given by the effective thickness t_{eff}) and the plane which produced the failure. Additionally, the load capacity obtained for the ductile mechanism is given as well, considering ($F_{EYM,Rope}$) and not considering (F_{EYM}) the rope effect. The ductile failure model (European Yield Model, EYM) is based on proposals from the practice literature (*Wallner-Novak et al.*, 2014; *Borgström and Fröbel*, 2019; *Bogensperger et al.*, 2010). The required embedment strength values are obtained from the declared characteristic density, and assumed the same for all layers, regardless of the angle between the force and the direction of the fibre.

Figure 4 presents a comparison of the model results with the experimental results. The figure shows the whole range of experimental results and the load capacities predicted from the brittle and ductile (without rope effect —yielding onset— and with rope effect —increased capacity after large displacements—) models. It has to be considered that in most of the tests, the yielding of the fastener was observed prior to the eventual brittle failure.

Statistical analyses using various metrics were performed as well (Table 5). The metrics are those used by *Cabrero and Yurrita* (2018) and allow a comprehensive

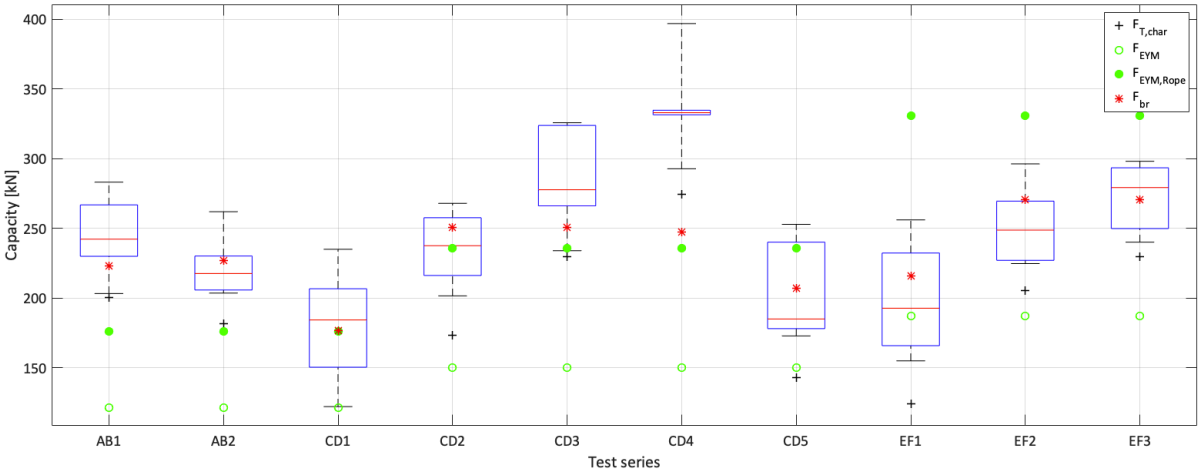

(a) Europe

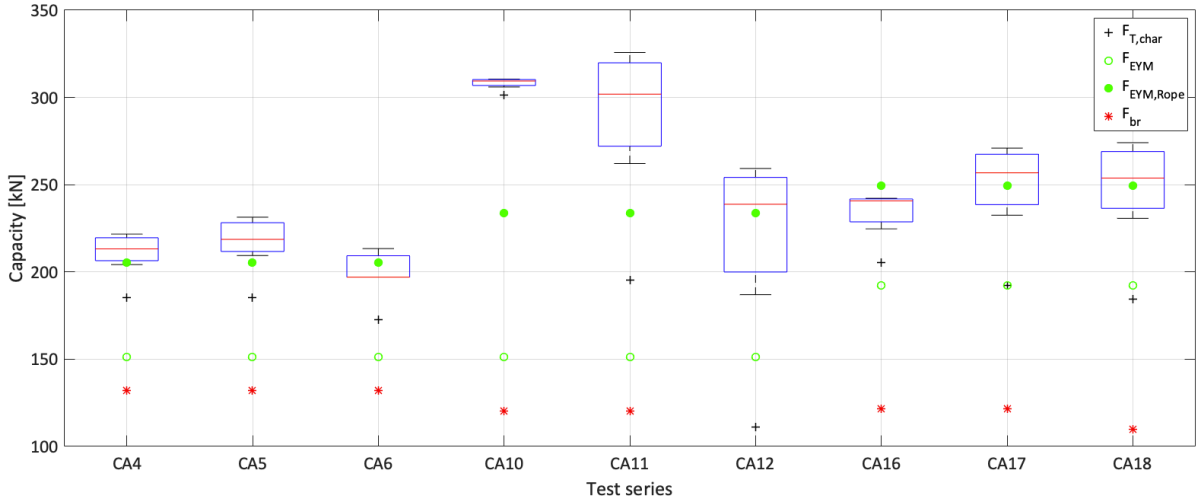

(b) Canada

Figure 4. Results from the models in comparison to the experimental results.

analysis of the model's response in different aspects. The overall performance is analyzed by the determination coefficient Q^2 (*Steyerberg et al.*, 2010; *Chirico and Gramatica*, 2011) (reliable threshold value 0.70, best values closest to 1) and the concordance correlation coefficient *CCC* (*Chirico and Gramatica*, 2011; *Chirico and Gramatica*, 2012; *Gramatica and Sangion*, 2016) (again, values close to 1 are best, recommended threshold value of 0.85). *CCC* is used as an alternative measure to Q^2, whose reliability has been questioned previously (*Golbraikh and Tropsha*, 2002; *Alexander et al.*, 2015). The ability to provide good correlation (without quantitative prediction) is assessed using the rank correlation coefficient *c* (*Alexander et al.*, 2015) (values closer to 1 are the best) and slope *m* of the linear fitting through the origin. In addition, mean relative error MRE (about 10% to be acceptable values) and associated standard deviation SD are observed.

Regarding the brittle model, the obtained values greatly differ between both test

Table 4. Results from the model and comparison to experimental results at the characteristic level (in brackets, corresponding ratio vs. experimental result).

Test	Experiment		Brittle model				EYM no rope	EYM + rope eff.
	$F_{t,k}$ [kN]	Fail.M.	F_{br} [kN]	Mode	Plane	t_{eff} [mm]	F_{EYM} [kN]	$F_{EYM,Rope}$ [kN]
Europe								
AB1	200.7	PS/RS	223.1 (1.11)	A	D	30.2	121.3 (0.60)	176.1 (0.88)
AB2	181.5	PS/RS	226.8 (1.25)	A	D	30.2	121.3 (0.67)	176.1 (0.97)
CD1	103.7	PS	176.4 (1.70)	C	D	30.2	121.3 (1.17)	176.1 (1.70)
CD2	173.5	PS	250.9 (1.45)	C	YR	44.8	150.0 (0.86)	235.9 (1.36)
CD3	229.6	PS/RS	250.9 (1.09)	C	YR	44.8	150.0 (0.65)	235.9 (1.03)
CD4	274.3	PS/RS	247.3 (0.90)	C	D	44.8	150.0 (0.55)	235.9 (0.86)
CD5	143.1	PS/RS	207.2 (1.45)	C	D	44.8	150.0 (1.05)	235.9 (1.65)
EF1	124.2	NT	215.7 (1.74)	E	YR	44.8	186.9 (1.50)	330.6 (2.66)
EF2	205.1	PS/RS	270.9 (1.32)	E	YR	64.0	186.9 (0.91)	330.6 (1.61)
EF3	229.7	PS/RS	270.9 (1.18)	E	YR	64.0	186.9 (0.81)	330.6 (1.44)
Canada								
CA4	185.3	EYM	132.1 (0.71)	C	YR	56.0	151.2 (0.82)	205.5 (1.11)
CA5	185.1	PS	132.1 (0.71)	C	YR	56.0	151.2 (0.82)	205.5 (1.11)
CA6	172.6	SS	132.1 (0.77)	C	YR	56.0	151.2 (0.88)	205.5 (1.19)
CA10	301.2	EYM	120.3 (0.40)	C	YR	68.7	151.2 (0.50)	233.8 (0.78)
CA11	195.2	PS	120.3 (0.62)	C	YR	68.7	151.2 (0.77)	233.8 (1.20)
CA12	111.0	SS	79.6 (0.72)	C	D	68.7	151.2 (1.36)	233.8 (2.11)
CA16	205.3	EYM	121.5 (0.59)	C	YR	64.0	192.4 (0.94)	249.4 (1.21)
CA17	192.1	EYM	121.5 (0.63)	C	YR	64.0	192.4 (1.00)	249.4 (1.30)
CA18	184.4	EYM	110.0 (0.60)	C	D	64.0	192.4 (1.04)	249.4 (1.35)

Failure modes: *PS, plug shear; RS, row shear (tearing); NT, net tension; SS, step shear; EYM, yielding of the fastener. Where two are indicated, both are observed in some specimens of the series.*
Mode (bottom failure plane location): *A, first layer; C, second layer; E, third layer.*
Plane legend*: D, bottom plane; YR, yielding of fastener + rolling shear; H, head plane.*

Table 5. Statistical analysis of the obtained results

	Overall performance		Correlation		Error	
	Q^2	*CCC*	*m*	*c*	*MRE*	*SD*
All tests	-1.21	0.18	0.90	0.22	0.33	0.19
Europe	-0.35	0.39	1.20	0.75	0.28	0.13
Canada	-2.34	0.09	0.59	0.05	0.38	0.23

campaigns. In the case of the European campaign, they are within the range of the obtained experimental values (Fig.4a), but fall outside and are much lower in the Canadian tests (Fig.4b). While the model overpredicts the European characteristic value, it clearly underpredicts the Canadian ones.

This different trend may be explained by two different aspects. The low number of replicates in the Canadian set may reduce the obtained characteristic value. However, this approach was preferred to apply those material properties used in practice. Additionally, the much different material values recommended in the literature (Table 3). Especially in the case of the shear strengths, both of which control the brittle capacity in the bottom plane or yielding rolling mechanism, the Canadian properties are lower (half or even more) than the European values.

As mentioned above, the applied Canadian properties were those for glulam since the Canadian values for CLT are even lower. If CLT values were applied, the reported brittle capacities would even be much lower (15% to 50% lower than those shown in Table 4, with ratios ranging from 19% to 53% of the experimental values). Moreover, having such a low tensile strength, the predicted failure plane changes: the head plane becomes the main failure mechanism, followed by the bottom plane.

The resulting failure mechanisms are either the bottom plane or the yielding-rolling limit mechanism. The latter is the most represented failure mode in the Canadian set (possibly due to the low rolling shear strength), while they are quite homogeneously reported in the European tests. No failure is related to the adjacent plane.

Most of the Canadian tests showed large ductilities, though they eventually failed in a brittle manner after a significant deformation. Unexpectedly, when assessing the models, the resulting brittle capacities are lower than the ductile values. Based on this, brittle failure would be expected, though it is not the case. Again, the low shear strengths in the standard may explain this fact.

As shown in Table 5, the prediction ability is quite low (negative Q^2, and very low *CCC* values). Although the quantitative prediction is poor (as shown by the performance and error metrics), the correlation of the model (that is, the ability to capture the trend) is quite good in the case of the European set. All the metrics worsen in the Canadian set which mostly failed with increased ductilities.

4 Conclusions

This work describes several tests on connections with laterally-loaded self-tapping screws on CLT plates subjected to parallel tension. This type of connection and internal force would be typical in the case of hold-downs, for example. It presents research carried out independently on the same topic in Europe and Canada, and thus allows for a more comprehensive perspective on the topic.

It was found that brittle failure typically occurs after the yielding of the fastener has already started. Quite low ductility values are typically observed, in the range of 1.5-2.5, which would make these types of connections not appropriate for their use in seismic areas, where higher local ductility would be desirable. However, it has been shown in the Canadian set how also ductile failure with ductility values over 4 can be reached as well. For connections with a reduced number of fasteners (as it is the case of the Canadian set), yield modes seem to govern.

The existing model, developed by *Zarnani and Quenneville* (2015), obtained quite scattered results in this work. One main reason is the noticeable differences among declared material properties between both regions. It must be stressed how the need for reliable material properties becomes (as always) a major task. Moreover, they should be obtained from tests in conditions comparable to those assumed in the model. Moreover, shown trends may be affected by the reliability of the characteristic level, due to the low number of replicates in the Canadian case.

Although the brittle model's prediction ability is quite low, its correlation is good, mostly in the case of the European set, which features most of the brittle failures with low ductility values. As it is a stiffness-based model and considers a main and a secondary failure mechanism, it becomes quite cumbersome. It demands the use of dedicated software (in our case, a MatLab script was produced, and validated with the original paper (*Zarnani and Quenneville*, 2015)). The development of simpler design models for practice is advisable.

CLT has become a major product in current timber construction. However, our current design methods for connections still demand improvements. Further work should be done to obtain a better prediction of both yield and brittle load-bearing capacities of CLT connections.

Acknowledgments

The European research has received support within ERA-NET Cofund ForestValue by MIZŠ, VINNOVA, FORMAS, STEM, BMLFUW, FNR and MINECO-AEI and has received funding from the European Union's Horizon 2020 research and innovation program under grant agreement N° 773324. The financial support provided by the Spanish Ministerio de Ciencia, Innovación y Universidades – Agencia Estatal de Investigación under contract PCI2019-103591 AEI is gratefully acknowledged.

This Canadian project was financially supported by the Canadian Forest Service of Natural Resources Canada, the Natural Sciences and Engineering Research Council of Canada and all industry partners of the Industrial Research Chair for Advanced Research in Timber Systems.

5 References

Alexander, D. L., A. Tropsha, and D. A. Winkler (2015). "Beware of R^2: Simple, Unambiguous Assessment of the Prediction Accuracy of QSAR and QSPR Models." In: *Journal of Chemical Information and Modeling* 55.7, pp. 1316–1322. DOI: 10.1021/acs.jcim.5b00206.

Asgari, H., T. Tannert, and C. Loss (2022). "Block tear-out resistance of CLT panels with single large-diameter connectors." In: *European Journal of Wood and Wood Products*. DOI: 10.1007/s00107-022-01809-3.

ASTM D5457-21a (2021). *Standard Specification for Computing Reference Resistance of Wood-Based Materials and Structural Connections for Load and Resistance Factor Design*.

ASTM D5764-97a (2018). *Standard Test Method for Evaluating Dowel-Bearing Strength of Wood and Wood-Based Products*. ASTM.

Azinović, B., J. M. Cabrero, H. Danielsson, and T. Pazlar (2022). "Brittle failure of laterally loaded self-tapping screw connections for cross-laminated timber structures." In: *Engineering Structures* 266, p. 114556. DOI: https://doi.org/10.1016/j.engstruct.2022.114556.

Bogensperger, T., T. Moosbrugger, and G. Schickhofer, eds. (2010). *BSPhandbuch, Holz- Massivbauweise in Brettsperrholz*. Verlag der Technischen Universität Graz.

Borgström, E. and J. Fröbel, eds. (2019). *The CLT Handbook*. First. Stockholm, Sweden: Swedish Wood.

Cabrero, J. M. and M. Yurrita (2018). "Performance Assessment of Existing Models to Predict Brittle Failure Modes of Steel-to-Timber Connections Loaded Parallel-to-Grain with Dowel-Type Fasteners." In: *Engineering Structures* 171. (INTER paper 51-7-12), pp. 895–910. DOI: 10.1016/j.engstruct.2018.03.037.

Chirico, N. and P. Gramatica (2012). "Real External Predictivity of QSAR Models. Part 2. New Intercomparable Thresholds for Different Validation Criteria and the Need for Scatter Plot Inspection." In: *Journal of Chemical Information and Modeling* 52.8, pp. 2044–2058. DOI: 10.1021/ci300084j.

Chirico, N. and P. Gramatica (2011). "Real External Predictivity of QSAR Models: How to Evaluate It? Comparison of Different Validation Criteria and Proposal of Using the Concordance Correlation Coefficient." In: *Journal of Chemical Information and Modeling* 51.9, pp. 2320–2335. DOI: 10.1021/ci200211n.

CSA O86-09 (2019). *Engineering Design in Wood*. Canadian Standards Association.

EN 12512 (2016). *EN 12512:2005, Timber Structures - Test Methods - Cyclic Testing of Joints Made with Mechanical Fastener*. CEN.

EN 14358 (2016). *Timber Structures - Calculation and Verification of Characteristic Values*. Tech. rep. CEN.

EN 26891 (1992). *Timber Structures -Joints Made with Mechanical Fasteners - General Principles for the Determination of Strength and Deformation Characteristics*.

ETA 11-0284 (2019). *Screws for Use in Timber Construction*.

ETA 12-0347 (2020). *Solid Wood Slab Element to Be Used as a Structural Element in Buildings*.

ETA 14-0349 (2020). *Solid Wood Slab Element to Be Used as a Structural Element in Buildings*.

Golbraikh, A. and A. Tropsha (2002). "Beware of Q^2!" In: *Journal of Molecular Graphics and Modelling* 20.4, pp. 269–276. DOI: 10.1016/S1093-3263(01)00123-1.

Gramatica, P. and A. Sangion (2016). "A Historical Excursus on the Statistical Validation Parameters for QSAR Models: A Clarification Concerning Metrics and Terminology." In: *Journal of Chemical Information and Modeling* 56.6, pp. 1127–1131. DOI: 10.1021/acs.jcim.6b00088.

Ni, C. and J. Niederwestberg (2022). *Investigation of brittle failure modes in self-tapping screw steel to wood connections parallel to the grain*. Tech. rep. 301014606. FPInnovation.

Schenk, M., C. Hübner, and J. M. Cabrero (2022). "Cross-Laminated Timber: A Survey on Design Methods and Concepts in Practice." In: *CivilEng* 3.3, pp. 610–629. DOI: 10.3390/civileng3030036.

Steyerberg, E. W., A. J. Vickers, N. R. Cook, T. Gerds, M. Gonen, N. Obuchowski, M. J. Pencina, and M. W. Kattan (2010). "Assessing the Performance of Prediction Models." In: *Epidemiology* 21.1, pp. 128–138. DOI: 10.1097/EDE.0b013e3181c30fb2.

Wallner-Novak, M., J. Koppelhuber, and K. Pock (2014). *Cross-Laminated Timber Structural Design*. proHolz Austria.

Yurrita, M. and J. M. Cabrero (2020). "New Design Model for Brittle Failure in the Parallel-to-Grain Direction of Timber Connections with Large Diameter Fasteners." In: *Engineering Structures* 217. (INTER paper 52-7-7), p. 110557. DOI: 10.1016/j.engstruct.2020.110557.

Yurrita, M. and J. M. Cabrero (2021). "Experimental analysis of plug shear failure in timber connections with small diameter fasteners loaded parallel-to-grain." In: *Engineering Structures* 238. (INTER paper 53-7-6), p. 111766. DOI: https://doi.org/10.1016/j.engstruct.2020.111766.

Yurrita, M., J. M. Cabrero, and E. Moreno-Zapata (2021). “Brittle Failure in the Parallel-to-Grain Direction of Timber Connections with Small Diameter Dowel-Type Fasteners: A New Design Model for Plug Shear.” In: *Engineering Structures* 241. (INTER paper 54-7-10), p. 112450. DOI: 10.1016/j.engstruct.2021.112450.

Zarnani, P. and P. Quenneville (2015). “New Design Approach for Controlling Brittle Failure Modes of Small-Dowel-Type Connections in Cross-laminated Timber (CLT).” In: *Construction and Building Materials* 100. (INTER paper 47-7-3), pp. 172–182. DOI: 10.1016/j.conbuildmat.2015.09.049.

Zarnani, P. and P. Quenneville (2014). “Wood Block Tear-out Resistance and Failure Modes of Timber Rivet Connections: A Stiffness-Based Approach.” In: *Journal of Structural Engineering* 140.2. (CIB-W-18 paper 45-7-1), p. 04013055. DOI: 10.1061/(ASCE)ST.1943-541X.0000840.